DAVINCI: A high-performance imager and integral field spectrograph for the W. M. Keck Observatory's next-generation adaptive optics facility

Sean M. Adkins[*a], James Bell[a], Al Conrad[a], Mike Fitzgerald[c], Renate Kupke[e], James E. Larkin[c], Lee Laiterman[e], Jim Lyke[a], Claire Max[d], Elizabeth McGrath[d], Mike Pollard[a], Sergey Panteleev[a], Sandrine Thomas[e], Peter Wizinowich [a]

[a] W. M. Keck Observatory, 65-1120 Mamalahoa Highway, Kamuela, HI, USA 96743;
[b] California Institute of Technology, 1200 E. California Blvd., Pasadena, CA 91125, USA
[c] University of California, Los Angeles, Box 951547, Los Angeles, CA 90095-1547
[d] University of California, Santa Cruz, 1156 High St., Santa Cruz, CA, USA 95062
[e] UCO/Lick Observatory, 1156 High St., Santa Cruz, CA, USA 95062

ABSTRACT

In this paper we report on the preliminary design of DAVINCI, the first light science instrument for the W. M. Keck Observatory's Next Generation Adaptive Optics facility. DAVINCI will provide imaging and coronagraphy at the diffraction limit from 0.7 μm to 2.4 μm over a field of ~30", and integral field spectroscopy with three sampling scales (10, 35, and 50 mas) and a field of view of 5.6" x 3" for the largest (50 mas) sampling scale. The science requirements for DAVINCI are discussed, followed by an examination of the challenges of designing the instrument within a strict limit on overall cost. The instrument's optical design and opto-mechanical configuration is described as well as the current performance predictions for the instrument.

Keywords: Adaptive Optics, Instrumentation, Image Slicer, Infrared, Integral Field Spectroscopy, Visible

1. INTRODUCTION

DAVINCI, the Diffraction limited Adaptive optics Visible and Infrared iNtegral field spectrograph and Coronagraphic Imager is the first light science instrument for the Next Generation Adaption Optics (NGAO) facility at the W. M. Keck Observatory (WMKO). NGAO[1] is a new LGS AO system for the Keck II telescope that will expand the range of science questions that can be addressed with LGS AO by providing near diffraction-limited performance in the near-IR (K band Strehl ~ 80%) over narrow fields (< 30" diameter) with modest correction down to ~0.7 μm, high sky coverage, improved sensitivity and contrast, and improved photometric and astrometric accuracy.

DAVINCI is a fully cryogenic instrument providing imaging and integral field spectroscopy at the diffraction limit over a wavelength range of 0.7 μm to 2.4 μm. The imaging mode has a fixed plate scale of 7 milliarcseconds (mas) and the field of view (FOV) is 28.7" x 28.7" using a Teledyne Hawaii-4RG detector with 4096 x 4096 pixels and a 2.5 μm cut-off wavelength. The imager provides a selectable coronagraph mask and a large selection of photometric, continuum, and narrowband filters. A tracking cold pupil mask is provided for H and K band observations, and an additional selection of pupil masks is provided for the shorter wavelength bands and for the coronagraph mode. A pupil imaging mode is also provided for alignment of the instrument with the AO system. The central portion (~6.5") of the DAVINCI FOV can be sent to the IFS, allowing simultaneous spectroscopy and imaging. The DAVINCI IFS mode provides 112 x 60 spatial samples over a wavelength range of 0.7 μm to 2.4 μm. Samplings scales of 10, 35, and 50 mas are provided, resulting in FOVs of 1.12" x 0.6", 3.92" x 2.1", and 5.6" x 3". Fixed gratings are provided for each wavelength range, operating in the first order near the blaze angle with R ~4,000. The IFS is optimized for narrow band observations (~5% bandpass) and uses a lenslet image slicer combined with novel reformatting optics to provide 6 virtual slits (680 pixels per spectra) on an H-4RG detector with a 2.5 μm cut-off wavelength.

[*] sadkins@keck.hawaii.edu; Phone: (808) 885-7887; Fax: (808) 885-4464; http://www.keckobservatory.org/

DAVINCI is being developed in collaboration with UCLA, UCSC, and UCO/Lick. DAVINCI successfully completed its preliminary design review as part of the NGAO preliminary design review in June 2010.

2. DAVINCI SCIENCE

The NGAO science requirements document (SRD) identifies five science cases as key science drivers. These science cases have been selected because they represent the strongest performance drivers for NGAO either because they are technically demanding or they represent high scientific priorities that we want the system to be capable of addressing in the most complete way possible. A number of additional science cases are also considered in the SRD, these are science drivers selected to ensure that the system is sufficiently flexible to address a broad range of science. The science drivers influence performance parameters such as wavelength coverage and FOV, and also add scope to the operational features and operating modes of the coordinated system of telescope, AO, and science instrument. The requirements for DAVINCI are derived from a combination of the NGAO key science drivers and science drivers. The process of developing the requirements for DAVINCI has taken into account not only the science requirements, but also a requirement to match the instrument to the capabilities and performance of the AO system, and to design and build the instrument within a strict cost cap. As is usually the case, once requirements were understood the next step was to develop the instrument's optical design, and iterate on that design to satisfy as many of the requirements as possible.

2.1 Imaging

DAVINCI's imager is designed for high throughput and good background suppression in order to take full advantage of the low backgrounds provided by the AO system. The combination of the AO system and DAVINCI imaging will support high accuracy relative photometry and high accuracy astrometry. To connect the science requirements to the imager's optical design we highlighted four performance parameters, all of which are related and balance of which holds the key to optimizing the design. These parameters are FOV, pixel scale, wavelength coverage, and sensitivity. Table 1 provides a matrix showing the science cases that drive the instrument requirements, and the values expected for each of the four performance parameters.

	Wavelength bands						**FOV**					**Sampling**	**Sensitivity**
Science Case	I	Z	Y	J	H	K	≤ 5"	≥ 10"	≥ 15"	≥ 20"	>20"		(5σ)
Measurements of General Relativity Effects in the Galactic Center*					**X**	**X**		**X**				≥ λ/2D	(see text)
Imaging and Characterization of Extrasolar Planets around Nearby Stars*			**X**	**X**	**X**	**X**	**X**					≥ λ/2D	20 min. for H = 25
Multiplicity of minor planets*	**X**	**X**	**X**	**X**	**X**	**X**	**X**					≥ λ/3D (J, H, K), λ/2D (I, Z)	1 hour for I = 28.8
Gravitational Lensing	**X**	**X**	**X**	**X**	**X**	**X**				**X**		≥ λ/2D	45 min for I = 23.5
Size, shape, and composition of minor planets		**X**	**X**	**X**	**X**	**X**	**X**					≥ λ/3D (J, H, K), λ/2D (I, Z)	1 hour for I = 28.8
Characterization of Gas Giant Planets				**X**	**X**	**X**					**X**	≥ λ/2D	(see text)
Resolved Stellar Populations in Crowded Fields	**X**	**X**		**X**	**X**	**X**			**X**			≥ λ/2D	1 hour for K = 27

* = NGAO key science driver

Table 1: Summary of the primary science driven parameters for DAVINCI imaging

In Table 1 the six wavelength bands are the photometric passbands for imaging (see Table 3 for the passband definitions). The FOVs in Table 1 refer to the diameter, and the sensitivity requirements in Table 1 are given for the cases that concern fainter targets. For the general relativity case and the study of the gas giant planets targets are brighter, and in some cases the problem becomes avoiding saturation at the longer wavelengths instead of obtaining adequate signal to noise ratio (SNR) for faint targets. For the longer infrared wavelengths the background contribution of the AO system and telescope does remain a consideration even for these brighter object science cases.

As shown in Table 1 several of these science cases identify the desirability of accessing wavelengths below 1 μm, either for specific diagnostic lines such as the Ca II triplet (~850 nm), or for the improved spatial resolution available at the shorter wavelengths. Initial evaluation of the I band for color-color diagrams indicates that extending coverage to this band will prove highly beneficial to the study of stellar populations.

Table 1 does not describe one other requirement that is important for the optical design of the imager, coronagraphy to support high contrast imaging. This requirement comes primarily from the science case for the detection and characterization of planets around nearby low mass stars. The high contrast performance requirements for DAVINCI imaging are:

1. $\Delta J = 8.5$ (or a contrast ratio of 4×10^{-4}) at 100 mas with a goal of $\Delta J = 11$ (4×10^{-5}) at 100 mas
2. $\Delta H = 10$ (or a contrast ratio of 1×10^{-4}) at 200 mas with a goal of $\Delta H > 5.5$ (6.3×10^{-3}) at 0.5"
3. $\Delta K = 10$ (or a contrast ratio of 1×10^{-4}) at 100 mas

These requirements reflect the goal for NGAO to support observations of Jupiter mass planets around nearby, young low mass stars, and brown dwarfs. This search space is distinct from the high contrast "extreme AO" systems in development which are specialized for finding young planets around bright, solar type stars at $I < 9$.

A number of the science cases also require high levels of astrometric and photometric performance from DAVINCI imaging. Photometric accuracy depends strongly on the stability of the point spread function (PSF) and NGAO is designed to provide a much more stable PSF. Studies of AO system performance suggest that effects due to imperfect correction of atmospheric turbulence and field dependent aberrations will be dominant over effects due the instrumentation. Motion within the instrument can contribute to PSF variability, but flexure is not expected to be a problem for DAVINCI as its structure is completely fixed, and there are no moving parts that can induce differential motion between parts of the optical path during an observation. Detector characteristics are expected to be the dominant factor in the instrument's photometric performance and these are well understood and largely controllable with good design practices.

The accuracy of position determination for a point source is ultimately determined by the width of the PSF and noise in the image due to photon statistics. As with photometric accuracy, the performance of the AO system, including the Strehl and the quality of the PSF both affect the SNR of the observation. In addition to sensitivity, the primary effect of the instrument on astrometric accuracy will be the amount of distortion present in the optical system. In addition to minimizing the presence of distortion through careful design and construction a high performance approach to measuring the distortion across the field of the imager will be required. Such characterization has been shown to have a significant impact on the astrometric accuracy that can be achieved with the existing Keck II AO system and the NIRC2 instrument. It should be noted that the Galactic center case makes the greatest demand on astrometric accuracy at < 0.1 mas, approaching the limit of what can be achieved due to photon statistics.

The pixel scale at the detector will determine the sampling of the delivered PSF and in turn will have an impact on both photometric and astrometric accuracy. The loss of spatial frequencies due to sampling will translate directly to a reduction in the accuracy with which the original flux distribution is represented in the sampled image, and will also result in an increase in position uncertainty for well resolved image features. Simulations have shown the benefits of increased sampling, especially for the J, H, and K bands where the high Strehls delivered by NGAO result in higher SNRs. This is particularly important for the minor planet science cases where objects are expected to be well resolved in the J and H bands.

One of the main issues for the trade off between FOV and image sampling is the selection of the pixel scale. For imaging that is background limited, coarser sampling, corresponding to larger pixels results in shorter maximum exposure times due to saturation on the background flux. Of course this effect is most significant in the near-IR bands due to OH lines and thermal sources. On the other hand, for read noise limited conditions finer sampling requires reading out more pixels, and increases the read noise contribution. To evaluate the relationship between pixel scale and sensitivity we calculated both the maximum exposure time to 50% of the detector's full charge storage capacity, and the point source magnitude at which an SNR of 5 achieved for pixel scales from 100 mas to 5 mas. The results of this analysis showed that with the reduced background achieved by cooling the AO system, the use of a high efficiency cold stop in DAVINCI, and read noise of 4 e- (demonstrated with the H-2RG using 16 Fowler samples[2]) pixel scales between 5 and 50 mas do not impact sensitivity in the J, H, and K bands. For the I, Z, and Y bands pixel scales between 7 and 20 mas have no impact on sensitivity. This suggests that there is no compelling sensitivity argument to guide the selection of pixel scale in the range of choices that address the diffraction limited sampling requirements for DAVINCI imaging, and also indicates that oversampling at longer wavelengths does not result in a penalty on SNR. On the other hand, within the infrared bands the sky background does limit the maximum exposure time before either the accumulated charge rises

to the point where the detector's response becomes non-linear or saturates. Here, smaller pixels are better, allowing significantly longer exposure times.

For reasons of complexity, optical performance, and cost we consider it desirable for the DAVINCI imaging mode to have a single fixed pixel scale. The NGAO science relay will offer an unvignetted field of view (FOV) covering 40" diameter. With a square detector, the square area that will fall entirely within a 40" FOV is 28.28" x 28.28". Given a 4096 x 4096 pixel detector, the corresponding pixel scale is 7 mas, resulting in a FOV of 28.7" x 28.7". A second candidate is an 8 mas scale, which provides a FOV of 32.8" x 32.8". As noted in Table 2, a number of the science cases require the imager to have a pixel scale that provides at more than 2 pixel sampling in the near-IR bands, and at least 2 pixel sampling in the Z and I bands. When the benefit of a larger field of view is considered it seems logical to consider either the 7 or 8 mas pixel scale as the best choice. When sampling vs. wavelength is considered it is desirable to choose the smaller scale since this will provide 2 pixel sampling over most of the I band. As a result we have selected the 7 mas pixel scale for the DAVINCI imager, providing a 28.7" x 28.7" FOV with an H-4RG detector.

2.2 Spatially Resolved Spectroscopy

An integral field spectrograph (IFS) is an ideal way to take advantage of the image quality offered by NGAO because of its ability to provide spatially resolved spectroscopy of diffraction limited images without suffering from losses due to a mismatch between a long slit and the shape of a complex object. IFS data can provide information essential for deconvolution of the point spread function (PSF) and offers a comprehensive tool for determining kinematics, mass distributions, and velocity dispersions.

DAVINCI's IFS capability is intended to meet the needs of a range of Galactic and extra galactic science observations. We have evaluated the key IFS performance parameters and determined that the parameters most critical to IFS science are wavelength coverage including the placement of the short wavelength cut-off, spectral resolution, FOV, spatial sampling, and sensitivity. Table 2 provides a matrix showing the needed values of these parameters for each of the science cases that represent the primary drivers of IFS performance for DAVINCI.

	Wavelength bands						**FOV**				**Sampling**	**Spectral**	**Sensitivity**
Science Case	I	Z	Y	J	H	K	≥ 2"	3"	4"	≥ 5"	**scale(s)**	**resolution**	(5σ)
Galaxy Assembly and Star Formation History*		**X**	**X**	**X**	**X**	**X**		**X**			50 to 100 mas (50% EE)	R ≥ 3000	K = 23.5 in 1 hour
Nearby Active Galactic Nuclei*		**X**	**X**	**X**	**X**	**X**			**X**		20 mas, λ/D in Z band	R ≥ 3000	SNR ≥ 30 in 1 hour at
Measurements of General Relativity Effects in the Galactic Center*					**X**	**X**				**X**	20 to 35 mas	R > 4000	K = 23.5 in 1 hour
Gravitational Lensing	**X**	**X**		**X**	**X**	**X**			**X**		≤ 50 mas	R ≥ 3000	45 min for I = 23.5

* = NGAO key science driver

Table 2: Summary of the primary science driven parameters for the DAVINCI IFS

While Table 2 makes reference to full wavelength bands for spectroscopy, our analysis indicates that the NGAO science cases requiring IFS observations are generally more concerned with obtaining a larger FOV than they are with full coverage of an entire near-IR or visible passband in one exposure. One of the key performance trades in IFS design is the FOV available for a given spatial sampling and spectral band pass. Covering a wider bandpass requires more detector pixels in the dispersion direction, so for a given detector size the number of spatial samples is determined by the bandpass. By using a series of narrowband filters such as 5% bandpass a 4k x 4k detector can meet the FOV and sampling requirements shown in Table 2. The suitability of ~5% bandpass can be demonstrated by considering examples from the science cases requiring IFS observations.

The Galactic Center case emphasizes the measurement of absorption lines in the H and K bands (such as HI absorption of Brγ emission at 2.166 μm) that fall within 5% band passes, while FOVs of at least 5" diameter are desirable for simultaneous measurements of multiple stars near the Galactic center to improve the strength of the orbital solutions. Measurements of GR effects at the Galactic center demand high SNR and diffraction limited spatial sampling. FOV and sensitivity are also important for population studies at the Galactic center[3].

Similarly, for emission line observations such as excitation temperatures, observations of molecular hydrogen emissions[4], and other spectral line features such as the CO bandheads, 5% band passes will suffice. For the galaxy

assembly and star formation case the primary requirement is sensitivity, while the FOV is less important provided that it is large enough to provide sufficient spatial pixels to accurately sample the sky background. For this science case since the targets are of known redshifts, and the key spectroscopic lines of interest for kinematics at redshifts of $1 < z < 3$ are observable within ~5% passbands in the near-IR (J, H, and K) bands, a narrow band pass is also satisfactory. In cases where observations of multiple lines are required, if the IFS field is suitably matched to the object size, such that the entire PSF of the object is imaged, then image motion can be detected and discounted using simple PSF fitting techniques[5]. This allows multiple narrow band exposures to be a practical alternative to a single broad band exposure.

Because the solution for black hole (BH) mass requires having a good model for the larger-scale structure of the galaxy the nearby AGN science case has a need for larger FOVs of 3" to 5" diameter, but again the observations required for the stellar and gas dynamics around the central black hole are based on absorption lines for stellar dynamics and emission lines for gas dynamics, all of which can be observed within 5% band pass or less in the Z through K bands. This science case in particular identifies the benefits of high angular resolution observations below 1 μm wavelength where the more compact PSF core at the shorter wavelength and the reduced sky background will enable BH detection over greater distances. Gravitational lensing also requires high SNR and an FOV of at least 4" to 5". The gravitational lensing science case also benefits from observations below 1 μm for access to diagnostic lines for the lensed source and for red shifted lines of the lensing galaxy.

3. DAVINCI DESIGN

DAVINCI must be designed and built in a cost capped environment, so at the outset we have adopted a design and build to cost approach supported by six principles:

1. Ensure that the instrument capabilities are well matched to key science requirements
2. Ensure that the instrument capabilities are matched to the AO system in order to maximize the science gains
3. Understand which requirements drive cost
4. Resist the temptation to add features
5. Maximize heritage from previous instruments
6. Evaluate ways to break the normal visible/near-IR paradigm of using different detectors in separate instruments

The design of DAVINCI is aimed at satisfying principles 1 and 2 as fully as possible and addressing the remaining principles with a clearly cost driven approach supported by sound engineering and technical decisions.

DAVINCI's design addresses principle 5 by adopting significant portions of its subsystem designs from other WMKO instruments, in particular MOSFIRE[2] and OSIRIS[6]. We address principal 6 by using substrate removed HgCdTe infrared focal plane arrays (FPAs). The substrate removed FPAs have good (~70%) QE down to 500 nm, and although the single CDS read noise is higher than typical science grade CCDs (~15 e^-/read for a Hawaii-2RG vs. 4 to 5 e^-/read for a deep depletion CCD) the low power dissipation of the FPA read out integrated circuit and the non-destructive pixel read out allows many Fowler or up the ramp samples and results in essentially the same readout noise levels for exposures where the exposure duration allows time for the required number of reads. The result is that while the QE of CCDs will be at least 20% higher at 1 μm and below, this seems to be the only penalty for not using a CCD below 1 μm.

To meet the cost requirements DAVINCI incorporates two instrument capabilities (imaging and spectroscopy) in a single cryogenic dewar with common fore-optics. The single dewar offers significant cost savings by eliminating the need to duplicate the dewar, cryogenic cooling system, and a number of control and supervisory systems such as temperature control and pressure monitoring. The IFS and imager are coaxial, resulting in the arrangement of the imager and IFS fields of view shown in Figure 1.

3.1 Opto-mechanical Design

The opto-mechanical arrangement of DAVINCI is shown in Figure 2, and the optical layout for the imager and IFS scale changer is shown in Figure 3. As shown in Figure 2 components are arranged on two levels, and the dewar is cylindrical with an outer diameter of ~2 m. The 120 mm diameter dewar entrance window is coupled by an insulated bellows to the cooled enclosure of the AO system, eliminating the need to provide a heating system for the window. The coronagraph mask wheel is located at the AO system focus inside the dewar and provides a selection of occulting spots, and a field

stop for the pupil imaging mode. The AO relay provides a telecentric output to DAVINCI with a focal ratio of f/46.38. Using a focal ratio of f/13.66 for the Keck telescope and a telescope plate scale of 0.727"/mm the resulting image scale at the focal plane of the AO relay is 0.727 x (46.38/13.66) or 2.47 mm/", resulting in a 40" focal plane approximately 99 mm in diameter.

The imager optical path consists of two pairs of off-axis parabolas (OAPs), all of which, along with the fold mirrors in the optical path are coated with bare gold. OAP1 (150 mm dia.) is located ~1 m after the focal plane as shown in Figure 3. This OAP has been optimized in off-axis angle and focal length to produce a high quality, 25mm pupil image at the cold stop. This was accomplished in Zemax by producing a configuration in which the primary mirror of the telescope was the object. Geometric rays from the primary mirror "object" were used to evaluate pupil image quality after passing through both the AO relay and DAVINCI's OAP1. Not surprisingly, to produce a high quality pupil image at the cold stop, the first OAP in DAVINCI must have an off-axis angle that is matched to that of the last OAP in the AO relay. This is because OAP4 of the AO relay and OAP1 of DAVINCI are acting as a nearly 1:1 relay between the tweeter mirror pupil plane (24 mm diameter) and the cold stop pupil plane (25 mm diameter) within the instrument. DAVINCI is provided with a cold stop or pupil mask matched to the Keck telescope primary mirror and central obscuration that will track the telescope pupil by rotating to compensate for the action of the AO system's k-mirror that de-rotates the sky image. The matched pupil mask is mounted in a wheel mechanism that also provides a selection of undersized pupil masks for the coronagraph and a 100% transmission circular mask for the short wavelength bands. A total of 45 filters for the imager and IFS modes are provided on wheels (15 per wheel plus an open position) located in the collimated space near the pupil. The pupil mask and filter wheels are shown at the center of Figure 2.

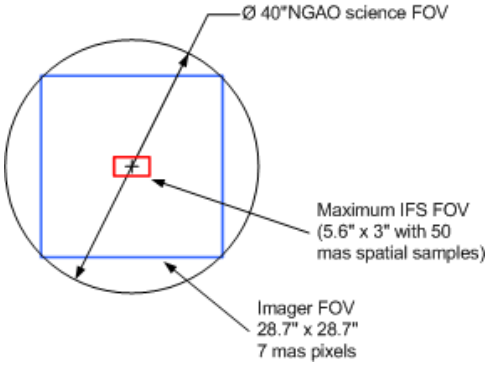

Figure 1: DAVINCI imager and IFS fields of view

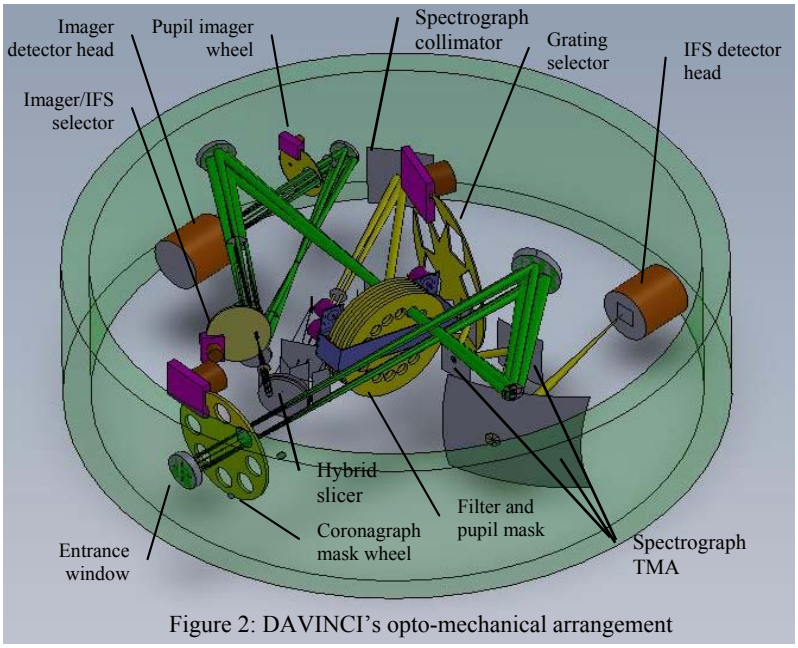

Figure 2: DAVINCI's opto-mechanical arrangement

Returning to Figure 3, OAP2 (110 mm dia.) is used to produce an intermediate focal plane near the IFS selection mirror (FM3). The distance between OAP1 and OAP2 is long, almost 1.5 m, because of the slow input f/#, the desired 25 mm pupil size at the cold stop, and the need for telecentricity on the input to the IFS, so to assist in packaging a 75 mm diameter fold mirror (FM1) is located 586 mm before the cold stop location. FM3 has a hole in it that allows light to pass to the IFS while allowing the rest of the field to pass on to the imager. The mirror can be rotated about its center which allows the hole to be moved out of the beam, sending the entire FOV to the imager. FM3 is titled at an angle of 15° and acts as one-half of a periscope that folds the beam down to a second level to aid in packaging the imager and IFS optical paths. A matching (15°) fold mirror completes the periscope to the second level. The vertical distance between levels is 127 mm.

To complete the scale change required by the imager's 7 mas pixel scale, a second OAP relay is used. OAP3 (90 mm dia.) produces a collimated beam in which a pupil image is formed one focal length away. This pupil image is not utilized, so its quality is not relevant. OAP4 (110 mm dia.) produces an image plane at the detector that is 61.4 mm in

diameter. A single plano-convex BaF_2 lens located ~5 mm from the detector (not shown in Figure 3) is used as a field flattener to compensate for the field curvature at the output of the AO system. The result is diffraction limited performance with a wavefront error of 27 nm at a radius of 10", and 58 nm at a radius of 14.4". The distortion is simple barrel distortion with a maximum of 4.2%.

In order to check pupil alignment between the AO relay and DAVINCI, a pupil imaging mode is provided. Pupil imaging is accomplished by placing a 400 mm, plano-convex BaF_2 lens 400 mm before the imager detector producing a pupil image ~10 mm in diameter. A pupil wheel mechanism (shown in Figure 2) is provided to insert the pupil imaging lens into the beam. The pupil imager is optimized for K band and requires a field stop 3 mm in diameter that is located in the coronagraph mask wheel. The imager detector head is based on the detector head developed for MOSFIRE, but adapted to the H-4RG. A focus adjustment is provided for initial set-up of the imager optical path when cold.

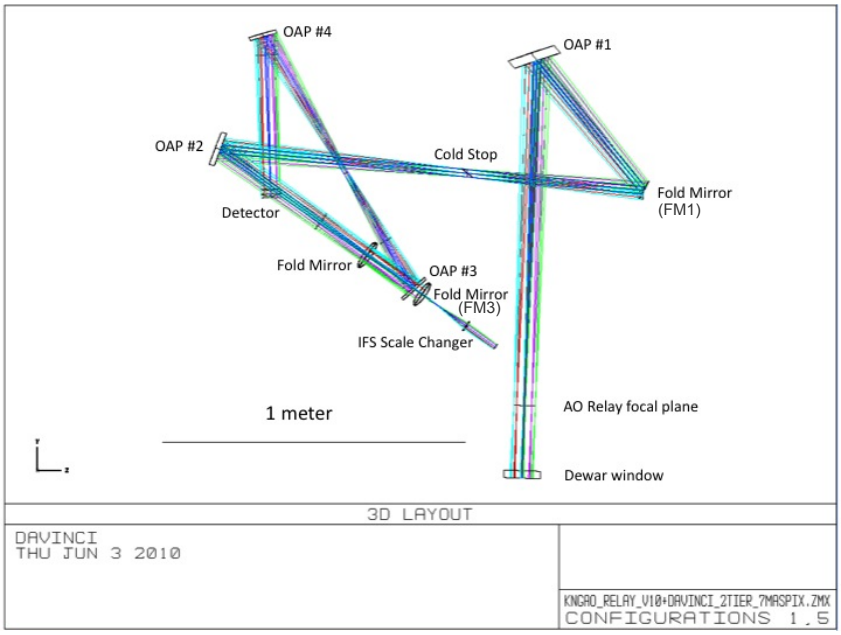

Figure 3: Imager and IFS scale changer optical layout

3.2 Integral Field Spectrograph

In the simplest form the IFS must accomplish three functions: image slicing, spectral dispersion, and detection of the dispersed spectra. Image slicing is a term used to describe the process of taking the spatial samples, effectively slicing the image into pixels, analogous to a CCD imager, but instead of becoming an intensity value each spatial pixel or "spaxel" is used to produce a spectrum. The size of the spatial pixel determines the spatial resolution of the image formed by the image slicer output. Just as with a CCD, where each pixel exhibits a characteristic point spread function (PSF), the image slicer also has a PSF determined by the performance of the image slicer's optical elements. In general the design of the spectrograph portion of an IFS instrument is similar to a conventional slit spectrograph for the same wavelength range.

There are three approaches to image slicing that have been used to build visible or infrared IFS instruments: fiber optics, mirrors and lenslets. The image slicer is placed at an image focal plane, often after scale changing optics which adjust the plate scale of the telescope or AO system to match the desired physical size of the image samples. To illustrate the basic operation of each concept, we will use a small scale example based on 16 spatial samples, arranged in a 4 x 4 grid.

Lenslet slicing[6],[7] shown in Figure 4, employs a two dimensional array of small lenses located at a focal plane to take each part of the image and focus it to a small pupil spot. The two dimensional pattern of spots effectively forms the entrance slit of a spectrograph, and the array of pupil spots is collimated and dispersed into spectra. Rotating the lenslet array slightly with respect to the dispersion axis of the grating eliminates overlap of the spectra within a column of lenslets. As a consequence of this rotation the spectra are staggered on the detector as shown in the figure. Lenslet slicers have the advantage that each spatial sample is completely independent in both the spectral and spatial directions. High quality arrays of lenslets with very well matched focal lengths and nearly perfect fill factors are routinely made using specialized manufacturing techniques. The difficulty with lenslet slicing is that due to the lenslet rotation adjacent

spectra are displaced with respect to each other on the detector in a pattern that repeats at the row pitch of the lenslets, this can result in bright features in one spectrum being next to fainter features in an adjacent spectrum. The displacement also leaves some of the detector area unused.

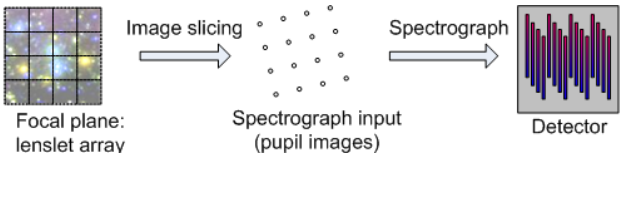

Figure 4: Lenslet slicer

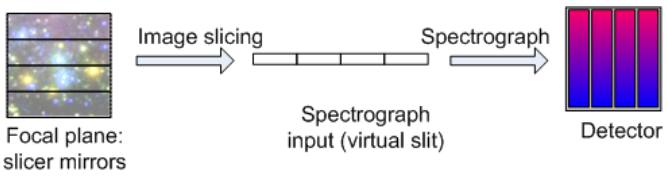

Figure 5: Mirror slicer

Mirror slicing[8],[9] shown in Figure 5, employs an array of mirrors located at a focal plane to deflect portions of the image light in different directions. Each mirror is equal to the physical width of a single spatial sample in one direction, and equal to the length of n spatial samples in the other direction, where n = 4 for the example of 4 x 4 spatial sampling. The light from each slicing mirror is collected by a second set of mirrors that format the slices into one or more rows in a virtual slit for the spectrograph. Flat or powered mirrors may be employed, and additional mirrors or lenses may be needed to place the pupil image at the correct conjugate in the spectrograph optical path. Mirror slicers have the advantage that the virtual slit approach can be more efficient in the use of the detector pixels. The disadvantages are greater light losses and additional sources of aberrations that can impact the quality of the spatial sampling. Light is lost at the input focal plane due the fact that the tilted mirrors move through focus, causing some light to be lost at each end of the long axis of each spatial sample. The mirrors are relatively small, typically between 0.3 and 0.5 mm in the narrow dimension. The mirrors only separate the samples in one dimension, so aberrations of the slicer mirror surfaces, as well as the aberrations through the spectrograph all contribute to loss of wavefront quality in the spatial direction.

For DAVINCI we have developed a new imager slicer concept we call the "hybrid slicer", illustrated in Figure 6. After an initial evaluation of the feasibility of achieving the desired FOV using either a mirror slicer or a lenslet array we realized that a system that uses mirrors to reformat the lenslet images into virtual slits might offer the best combination of low wavefront error and efficient detector utilization.

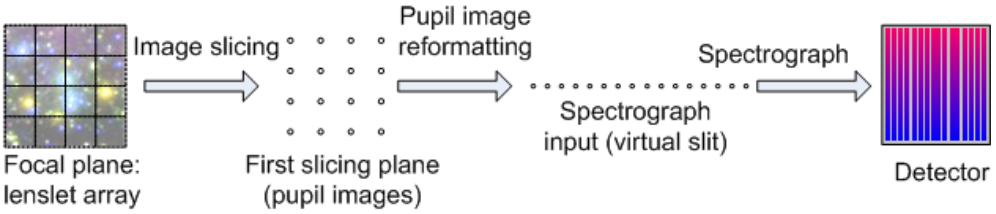

Figure 6: Hybrid slicer

In the hybrid slicer a lenslet array forms a series of pupils that are then reformatted by a slicer stack and a series of pupil mirrors into rows of virtual slits at the entrance of the spectrograph. This design has the advantage of maintaining the well isolated spatial samples of the lenslet array design all the way to the detector and avoids the problem of overlap between staggered spectra on the detector. A hybrid slicer will require a greater distance between the pupil image plane and the lenslet array to allow for mirrors to redirect columns of pupil images to the formatting optics. However, the lenslet focal length is not constrained by the need to achieve a small pupil image size in order to fit the desired number of lenslet images between the row pitch that results from rotation of the lenslet array in a pure lenslet slicer.

As shown in Figure 3, after FM3 (the IFS/imager selection mirror) the light going to the IFS enters a scale changing relay with three selectable scales. The relay contains three pairs of interchangeable lenses, mounted in wheels, relaying the image over a constant distance but with different magnifications. This arrangement is very similar to that used in the OSIRIS instrument[6]. Each pair of lenses are made from BaF_2 and each relay images the central portion of the intermediate focus onto the IFS lenslet array which consists of 112 x 60 lenslets on a 250 μm pitch. This is followed by the reformatting system used to produce the virtual slits, shown in Figure 7.

The hybrid slicer consists of a refractive field magnifier consisting of two doublets that enlarges the array of pupil images from the lenslet, providing the space needed to perform the reformatting. A tent mirror splits the field into two halves on the long axis, and each half is then sent to identical arrays of reformatting mirrors. All of the reflective optics in the hybrid slicer will be coated with bare gold. The reformatting mirrors are arranged so that each half of the field is effectively split into two halves on the short axis, resulting in 4 quadrants of 56 x 30 lenslets as illustrated in Figure 8.

The slicing mirrors are illustrated in Figure 9. The first set of reformatting mirrors, M1, is an array of spherical mirrors similar to a conventional mirror slicer and which reformats the rows of pupil images from the lenslet into three staggered lines consisting of 10 sections of 56 lenslets in a staggered line as shown in Figure 8. The second set of reformatting mirrors, M2, consists of three sets of 10 spherical mirrors each set of which aligns the staggered lines corresponding to 10 sections of 56 lenslets to form a virtual slit of 560 pupil images. For clarity only one set of M1/M2 mirrors covering one quadrant of the FOV are shown in Figure 9. By repeating this process for the other 3 quadrants we obtain six virtual slits each consisting of 1120 pupil images. The M1 and M2 mirrors not only reformat the lenslet array in each quadrant but also de-magnify the field by 12.5 x to achieve a reasonable size for the pseudo-slits. M1 and M2 are separated by the sum of their focal lengths, preserving the telecentricity at the slit plane. The beams are collimated in the M1 to M2 space to keep the beam foot print small at M2. This is achieved by placing M1 at one focal distance from the intermediate focal plane.

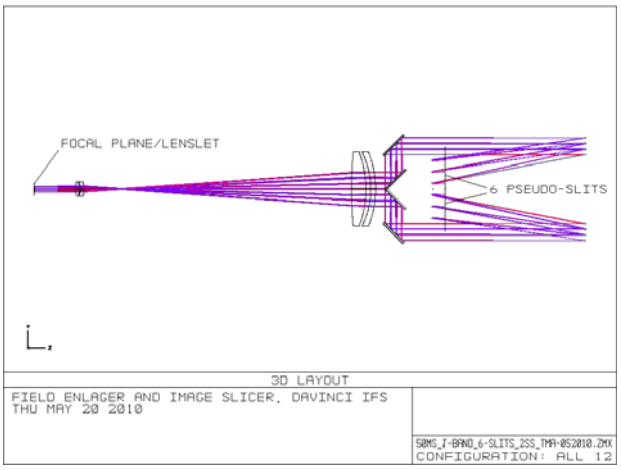

Figure 7: Hybrid slicer optical layout

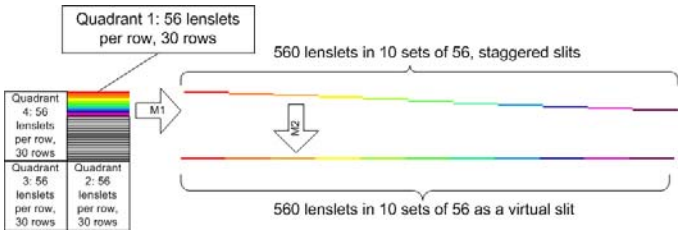

Figure 8: IFS virtual slit reformatting process

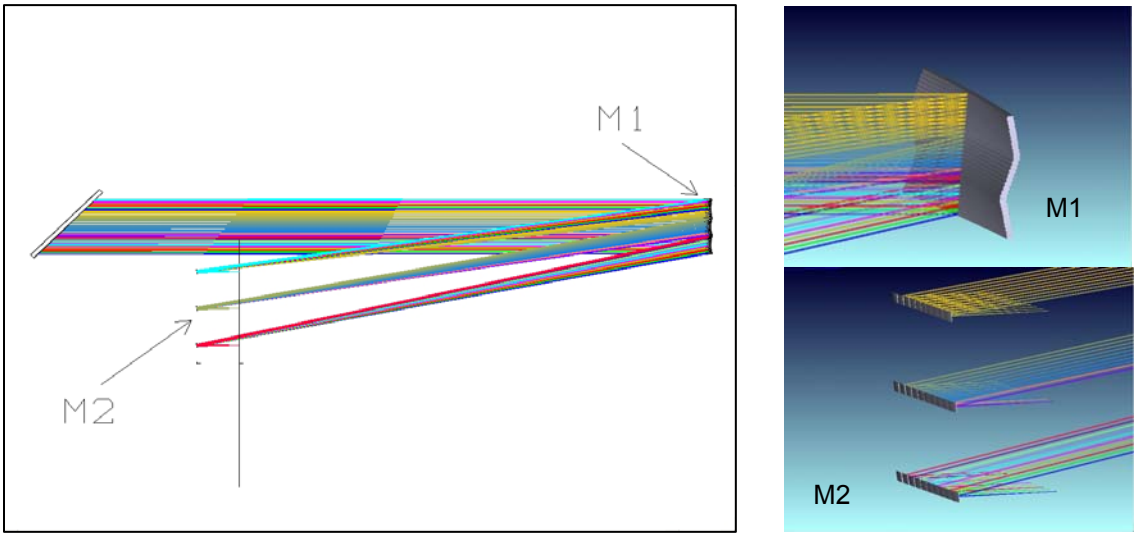

Figure 9: Hybrid slicer reformatting mirrors

The six virtual slits at the output of the hybrid slicer are collimated by a single aspheric collimating mirror followed by a grating wheel carrying 7 gratings (1 for each wavelength band, I, Z, Y, J, and H, and 2 for K band) and a plane mirror as shown in Figure 2. A three mirror anastigmat (TMA) forms the camera and this is followed by a second detector head (also based on the MOSFIRE design) using an H-4RG detector. The DAVINCI TMA design is based on the IRIS TMA design by Brian Bauman[10]. The collimator and camera mirrors are also coated with bare gold. The optical layout and

predicted performance of the spectrograph collimator and camera are shown in Figure 10. The design meets the requirement for 80% ensquared energy in a 2 pixel box.

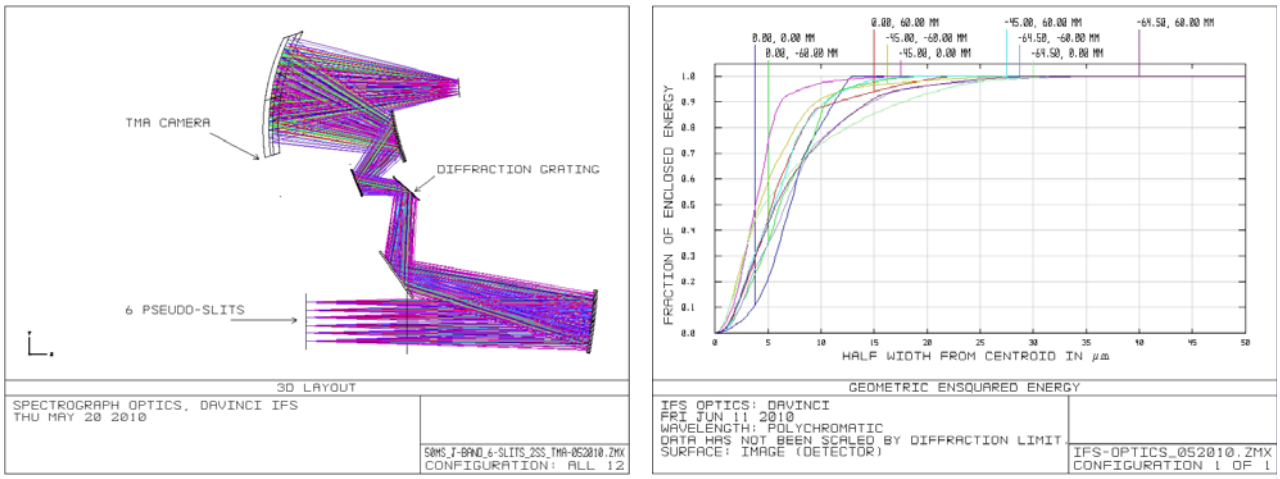

Figure 10: Optical layout for the IFS collimator and camera (left) and the ensquared energy at the detector (right)

We have evaluated the effects of diffraction in the hybrid slicer using physical optics propagation in Zemax. The effect of diffraction is to cause a small portion of the light (< 3% for the largest sampling scale of 50 mas) to be lost after M1 in the reformatting optics. Proper baffling will prevent this light from adding unwanted background to the spatial samples.

4. PERFORMANCE ESTIMATES

4.1 Imager

The imager photometric passbands, zero points, and background predictions for DAVINCI imaging are shown in Table 3. The sensitivity predictions for DAVINCI imaging are shown in Table 4. The background predictions are based on a cooled AO system operating at a temperature of -15 °C and emissivity for the LGS observing mode assuming degraded optical transmission due to dust and aging of coatings. The background predictions also include the effects of moonlight (50% dark time) in the I and Z band. The average transmission in each passband is used for the atmosphere, telescope, AO system, and DAVINCI's imaging optical path which is described in the next section of this paper. Thermal background within DAVINCI is suppressed by operating the instrument at 120 K in a vacuum dewar.

Photometric Passband	Cut-on, nm	Cut-off, nm	CWL, nm	Zero point	Background, mag./sq. arcsecond
I band photometric	700	853	776.5	27.34	19.33
Z band photometric	818	922	870	27.16	18.45
Y band photometric	970	1070	1020	26.92	17.28
J band photometric	1170	1330	1250	26.96	16.04
H band photometric	1490	1780	1635	26.96	13.76
K' band photometric	1956	2291	2124	26.39	13.86
K band photometric	2030	2370	2200	26.35	13.42

(Cut-on and cut-off wavelengths at 50% transmission points, CWL = central wavelength,
Table 3: Zero points and background magnitudes for DAVINCI imaging

The zero point magnitudes and the sensitivity predictions are based on the detector characteristics summarized in Table 5. Sensitivities are calculated assuming the delivered NGAO Strehl based on 170 nm wavefront error. The required aperture for a diffraction limited image is assumed to be that needed for a well compensated image[11], i.e. a diameter equal to $2\lambda/D$ where D is the diameter of the telescope aperture, and λ is the long wavelength cut-off in the passband of interest. It should be noted that the four 120 s exposures for I and Z band in Table 4 are not background limited. The Z band exposures need to be increased to 1200 s per frame to become background limited and the I band exposures need to be increased to 1800s to become background limited.

Photometric Passband	Ave. Strehl (170 nm wavefront error)	Time per exposure	5σ mag.	Time for single exposure to background limit, mag. = 27
I band photometric	15%	120 s	27.1	2.2 h
Z band photometric	22%	120 s	27.05	1.3 h
Y band photometric	33%	900 s	28.05	2400 s
J band photometric	47%	900 s	27.65	720 s
H band photometric	65%	900 s	26.6	100 s
K' band photometric	77%	900 s	26.25	180 s
K band photometric	79%	900 s	26	120 s

(5σ magnitudes are for 4 co-added exposures)
Table 4: DAVINCI imaging sensitivity

Parameter	Min. Value	Notes
Dark Current	0.01 e^-/s	Median dark current of all imaging pixels
Charge Storage Capacity	100,000 e^-/pixel	Array average number of electrons where the photon transfer curve first deviates from a straight line
Read Noise	15 e^-/pixel	Per CDS read
Quantum Efficiency	0.80 0.75 0.70	970 to 2400 nm 850 to 970 nm 700 to 850 nm

Table 5: Hawaii-4RG performance parameters

4.2 IFS Sensitivity

Zero points and background predictions for representative DAVINCI IFS passbands are shown in Table 6. Sensitivity and background predictions for DAVINCI in comparison with OSIRIS[6] using the 35 mas spatial sampling scale in the J, H, and K bands are shown in Table 7. Making sensitivity predictions for an IFS is more complex than for an imager since each spatial sample produces a spectrum that is spread over a number of detector pixels, and systematic effects in the data reduction process play a role in the resulting SNR. For these predictions we have computed the backgrounds, zero points and sensitivity on a per spatial sample basis, assuming a narrowband format for each IFS (856 pixels per spectra on average for OSIRIS, and 1360 pixels per spectra for DAVINCI).

Passband	Cut-on, nm	Cut-off, nm	CWL, nm	Zero point	Background, mag./sq. arcsecond
Ia narrow band spectroscopic	700	784	742.1	25.71	19.57
Za narrow band spectroscopic	855	962	908.6	26.14	17.33
Yb narrow band spectroscopic	1045	1120	1083	25.56	16.96
Jb narrow band spectroscopic	1200	1310	1255	25.62	15.83
Hc narrow band spectroscopic	1650	1746	1698	24.76	13.76
K' band spectroscopic*	1956	2291	2124	25.45	14.08
Kc narrow band spectroscopic	2200	2310	2255	24.16	13.72

(Cut-on and cut-off wavelengths at 50% transmission points, CWL = central wavelength,
** = no K' filter is planned for the IFS mode, values for reference only)*
Table 6: Zero points and background magnitudes for DAVINCI IFS

Band DAVINCI/OSIRIS	Strehl		Point source magnitude (SNR = 5)		Background (mag./square arc second)	
	DAVINCI	OSIRIS	DAVINCI	OSIRIS	DAVINCI	OSIRIS
Jb/Jn2	47%	3%	26.1	20.97	15.83	15.50
Hc/Hn4	65%	12%	24.8	22	13.76	13.92
Kc/Kn4	79%	31%	23.9	21.75	13.72	12.27

Table 7: DAVINCI and OSIRIS sensitivity and background comparison

5. CONCLUSIONS

We have developed a design for an imager and IFS that meets the science requirements for NGAO within the cost cap. The hybrid slicer design has been developed to a preliminary design level and quotations obtained for optically contact

bonded Zerodur mirror assemblies for the reformatting mirrors, and also for diamond turned aluminum mirror assemblies. Simulations of the virtual slit design indicate that the calibration is well behaved and somewhat simpler that a pure lenslet design and the additional throughput loss of ~ 10% is more than offset by the improved noise performance due to a reduction in the offsets and overlap between the spectra from each spatial sample. Further work is required to confirm these initial performance estimates using simulated data with a data reduction pipeline.

ACKNOWLEDGEMENTS

The W. M. Keck Observatory is operated as a scientific partnership among the California Institute of Technology, the University of California, and the National Aeronautics and Space Administration. The Observatory was made possible by the generous financial support of the W. M. Keck Foundation. This material is based upon work supported by AURA through the National Science Foundation under Scientific Program Order No. 5 as issued for support of the Telescope Systems Instrumentation Program (TSIP), in accordance with Proposal No. AST-0335461 submitted by AURA. We also wish to thank the Thirty Meter Telescope's IRIS team led by James Larkin and Anna Moore for valuable advice and for the use of the TMA design for IRIS.

REFERENCES

[1] Wizinowich, P. L., Adkins, S. M., Bell, J. M., Chin, J. Y. C., Stalcup, Jr., T. E., Johansson, E. M., Johnson, J. M., Medeiros, D. W., Morrison, D., Neyman, C. R., Panteleev, S., Pollard, M., Wetherell, E., Gavel, D. T., Max, C. E., Kupke, R., Reinig, M. R., McGrath, E. J., Lockwood, C., Dekany, R. G., Bouchez, A. H., Velur, V. N., & Marchis, F. "W. M. Keck Observatory's next generation adaptive optics facility", In *Proceedings of the SPIE 7736*, 19. (2010).

[2] McLean, I. S., Steidel, C. C., Epps, H. W., Matthews, K. Y., & Adkins, S. M. "Design and development of MOSFIRE: the multi-object spectrometer for infrared exploration at the Keck Observatory", In *Proceedings of the SPIE 7735*, 49. (2010).

[3] Lu, J. R., Ghez, A. M., Hornstein, S. D., Morris, M. R., Becklin, E. E., & Matthews, K. "A disk of young stars at the galactic center as determined by individual stellar orbits", *The Astrophysical Journal, 690*(2), 1463-1487. (2009).

[4] Beck, T.L., McGregor, P. J., Takami, M., & Pyo, T. "Spatially resolved molecular hydrogen emission in the inner 200 AU environments of classical T Tauri stars", *The Astrophysical Journal, 676*(1), 472-489. (2008).

[5] Roth, M. M. "PSF-fitting techniques for crowded field 3D spectroscopy", *New Astronomy Reviews 49*, 573-581. (2006).

[6] Larkin, J., Barczys, M., Krabbe, A., Adkins, S., Aliado, T., Amico, P., Brims, G., Campbell, R., Canfield, J., Gasaway, T., Honey, A., Iserlohe, C., Johnson, C., Kress, E., LaFreniere, D., Lyke, J., Magnone, K., Magnone, N., McElwain, M., Moon, J., Quirrenbach, A., Skulason, G., Song, I., Spencer, M, Weiss, J., & Wright, S. "OSIRIS: a diffraction limited integral field spectrograph for Keck", *New Astronomy Reviews 50*(4-5), 362-364. (2006).

[7] Bacon, R., Adam, G., Baranne, A., Courtes, G., Dubet, D., Dubois, J. P., Emsellem, E., Ferruit, P., Georgelin, Y., Monnet, G., Pecontal, E., Rousset, A., & Say, F. "3D spectrography at high spatial resolution: I. Concept and realization of the integral field spectrograph TIGER", *Astronomy and Astrophysics Supplement 113*, 347-357. (1995).

[8] Content, R. (1997). "New design for integral field spectroscopy with 8-m telescopes", In *Proceedings of the SPIE 1872*, 1295-1305. (1997).

[9] Eikenberry,S. S., Elston, R., Guzman, R., Raines, S. N., Julian, J., Gruel, N., Boreman, G., Hoffmann, J., Rodgers, M., Glenn, P., Hull-Allen, G., Myrick, B., Flint, S., & Comstock, L. "FISICA: The Florida image slicer for infrared cosmology and astrophysics", *New Astronomy Reviews 50*(4-5), 365-369. (2006).

[10] Moore, A. M., Bauman, B. J., Barton, E. J., Crampton, D., Delacroix, A., Larkin, J. E., Simard, L., & Wright, S. A. "The infrared imaging spectrograph (IRIS) for TMT: Spectrograph design", In *Proceedings of the SPIE 7735*, 87. (2010).

[11] Hardy, J. W. "*Adaptive optics for astronomical telescopes*", Oxford, UK: Oxford University Press. (1998).